

Solitary Wave Complexes in Two-Component Condensates

Natalia G. Berloff

Department of Applied Mathematics and Theoretical Physics, University of Cambridge, Cambridge, CB3 0WA, United Kingdom
(Received 4 December 2004; published 28 March 2005)

Axisymmetric three-dimensional solitary waves in uniform two-component mixture Bose-Einstein condensates are obtained as solutions of the coupled Gross-Pitaevskii equations with equal intracomponent but varying intercomponent interaction strengths. Several families of solitary wave complexes are found: (1) vortex rings of various radii in each of the components; (2) a vortex ring in one component coupled to a rarefaction solitary wave of the other component; (3) two coupled rarefaction waves; (4) either a vortex ring or a rarefaction pulse coupled to a localized disturbance of a very low momentum. The continuous families of such waves are shown in the momentum-energy plane for various values of the interaction strengths and the relative differences between the chemical potentials of two components. Solitary wave formation, their stability, and solitary wave complexes in two dimensions are discussed.

DOI: 10.1103/PhysRevLett.94.120401

PACS numbers: 03.75.Lm, 05.45.-a, 67.40.Vs, 67.57.De

Solitons and solitary waves represent the essence of many nonlinear dynamical processes from motions in fluids to energy transfer along biomolecules, as they define possible states that can be excited in the system. These are localized disturbances of the uniform field that are form preserving and move with a constant velocity. The nonlinear Schrödinger (NLS) equation $i\psi_t + \nabla^2\psi + \gamma|\psi|^2\psi = 0$ is a canonical and universal equation which is of major importance in continuum mechanics, plasma physics, nonlinear optics, and condensed matter [where it describes the behavior of a weakly interacting Bose gas and known as the Gross-Pitaevskii (GP) equation]. The reason for its importance and ubiquity is that it describes the evolution of the envelope ψ of an almost monochromatic wave in a conservative system of weakly nonlinear dispersive waves. Similarly, systems of the coupled NLS equations have been used to describe motions and interactions of more than one wave envelopes in cases when more than one order parameter is needed to specify the system. The coupled NLS equations have been receiving a lot of attention with recent experimental advances in multicomponent Bose-Einstein condensates (BECs). BECs can excite various exotic topological defects and provide a perfect testing ground to investigate their physics, because almost all parameters of the system can be controlled experimentally. Topological defects in two-component BECs have been predicted theoretically, but there is still no understanding of what the complete families of these defects and solitary waves are, nor of their properties, formation mechanisms and dynamics. It has also been suggested [1] that multicomponent BECs offer the simplest tractable microscopic models in the proper universality class of cosmological systems and solitary waves in multicomponent BECs may have their analogs among cosmic strings. The goal of this Letter is to find and characterize the families of solitary waves that exist in systems of the coupled NLS equation in three dimensions. The implications of these solitary waves are wide ranging, but they will be discussed in the context of two-component BECs.

The simplest example of a multicomponent system is a mixture of two different species of bosons, for instance, ^{41}K - ^{87}Rb [2]. Since alkali atoms have spin, it is also possible to make mixtures of the same isotope, but in different internal spin states, for instance, for ^{87}Rb [3]. The multicomponent BECs are far from being a trivial extension of a one-component BEC and present novel and fundamentally different scenarios for their excitations and ground state [4]. The theory for a mixture of two different bosonic atoms can be developed similar to that for a one-component condensate whose equilibrium and dynamical properties can be accurately described by the GP equation [5] for the wave function ψ of the condensate

$$i\hbar \frac{\partial \psi(\mathbf{r}, t)}{\partial t} = -\frac{\hbar^2}{2m} \nabla^2 \psi(\mathbf{r}, t) + V_0 |\psi(\mathbf{r}, t)|^2 \psi(\mathbf{r}, t), \quad (1)$$

where m is the mass of the atom, $V_0 = 4\pi\hbar^2 a/m$ is the effective interaction between two particles, and a is the scattering length. The GP model has been remarkably successful in predicting the condensate shape in an external potential, the dynamics of the expanding condensate cloud, and the motion of quantized vortices. The family of the solitary waves for (1) was numerically obtained in [6]. In a momentum-energy ($p\mathcal{E}$) plot, the sequence of solitary waves has two branches meeting at a cusp where p and \mathcal{E} simultaneously assume their minimum values. For each p in excess of the minimum p_c , two values of \mathcal{E} are possible, and $\mathcal{E} \rightarrow \infty$ as $p \rightarrow \infty$ on each branch. On the lower (energy) branch the solutions are asymptotic to large circular vortex rings. As p and \mathcal{E} decrease from infinity on this branch, the solutions begin to lose their similarity to vortex rings. Eventually, for a momentum p_0 slightly in excess of p_c , they lose their vorticity, and thereafter the solutions may better be described as “rarefaction waves”. The upper branch solutions consist entirely of these waves and, as $p \rightarrow \infty$, they asymptotically approach the rational soliton solution of the Kadomtsev-Petviashvili type I equation.

For two components, described by the wave functions ψ_1 and ψ_2 , with N_1 and N_2 particles, respectively, the GP

equations become (see, e.g., Refs. [4])

$$\begin{aligned} i\hbar \frac{\partial \psi_1}{\partial t} &= \left[-\frac{\hbar^2}{2m_1} \nabla^2 + V_{11}|\psi_1|^2 + V_{12}|\psi_2|^2 \right] \psi_1, \\ i\hbar \frac{\partial \psi_2}{\partial t} &= \left[-\frac{\hbar^2}{2m_2} \nabla^2 + V_{12}|\psi_1|^2 + V_{22}|\psi_2|^2 \right] \psi_2, \end{aligned} \quad (2)$$

where m_i is the mass of the atom of the i th condensate, and the coupling constants V_{ij} are proportional to scattering lengths a_{ij} via $V_{ij} = 2\pi\hbar^2 a_{ij}/m_{ij}$, where $m_{ij} = m_i m_j / (m_i + m_j)$ is the reduced mass.

Two-component one-dimensional BECs have recently been considered and various structures have been identified [7] such as bound dark-dark, dark-bright, dark-antidark, dark-gray, etc., complexes. In higher dimensions, domain walls [8] and skyrmions (vortons) [9] have been identified by numerical simulations. Numerical simulations of two-dimensional rotating two-component condensates were performed [10] and the structure of vortex states were investigated. A phase diagram in the intercomponent-coupling versus rotation-frequency plane revealed rich equilibrium structures such as triangular, square, and double-core lattices and vortex sheets. These simulations give a taste of a rich variety of static and dynamic phenomena in multicomponent condensates. One would expect the existence of various other families of solutions many of which have not yet been detected.

In what follows I determine the families of three-dimensional axisymmetric solitary wave solutions that move with a constant velocity U in *uniform* two-component mixture BECs. The trap geometry, relevant to experiments, introduces a harmonic-oscillator potential in (2) together with additional parameters, places restrictions on studies of solitary waves and their stability and is irrelevant in the view of our interest to effects that occur in large systems. Also, I believe that additional physical mechanisms should be introduced only *after* simpler models are well understood. Nevertheless, the results I obtain will be relevant to experiments with a sufficiently shallow trap, so the linear dimensions of the trap are much larger than the healing length. To reduce the number of parameters in the system, I will assume that the intracomponent scattering lengths and masses of individual components in the mixture are equal, so that $m_i = m$ and $a_{ii} = a$, but the intercomponent scattering lengths differ from a .

To find axisymmetric solitary wave solutions moving with velocity U in positive z direction, I solve

$$\begin{aligned} 2iU \frac{\partial \psi_1}{\partial z} &= \nabla^2 \psi_1 + (1 - |\psi_1|^2 - \alpha |\psi_2|^2) \psi_1, \\ 2iU \frac{\partial \psi_2}{\partial z} &= \nabla^2 \psi_2 + (1 - \alpha |\psi_1|^2 - |\psi_2|^2 - \Lambda^2) \psi_2, \\ \psi_1 &\rightarrow \psi_{1\infty}, \quad \psi_2 \rightarrow \psi_{2\infty}, \quad \text{as } |\mathbf{x}| \rightarrow \infty, \end{aligned} \quad (3)$$

where a dimensionless form of (2) is used such that the distances are measured in units of the correlation (healing)

length $\xi = \hbar/\sqrt{2m\mu_1}$, the frequencies are measured in units $2\mu_1/\hbar$ and the absolute values of the fields $|\psi_1|^2$ and $|\psi_2|^2$ are measured in units of particle density $n = \mu_1/V_{11}$. Also present in (3) are the parameter of the intercoupling strength $\alpha = V_{12}/V_{11}$ and the measure of asymmetry between chemical potentials $\Lambda^2 = (\mu_1 - \mu_2)/\mu_1$ (where we assume that $\mu_1 > \mu_2$).

The dispersion relation between the frequency ω and the wave number k of the linear perturbations ($\propto \exp[i\mathbf{k} \cdot \mathbf{x} - i\omega t]$) around homogeneous states $\psi_{i\infty}$ is obtained as

$$[4\omega^2 - k^2(k^2 + 2\psi_{1\infty}^2)][4\omega^2 - k^2(k^2 + 2\psi_{2\infty}^2)] = Pk^4, \quad (4)$$

where $P = 4\alpha^2 \psi_{1\infty}^2 \psi_{2\infty}^2$. The condition of dynamic stability $\omega(k) > 0$ gives $\alpha^2 < 1$. If $\alpha < -1$, the gas is unstable to formation of a denser state containing both components, while if $\alpha > 1$, then the two components will separate. In what follows I will consider $0 < \alpha < 1$. Note that the use of Feshbach resonances to vary the interactions between atoms makes this entire range of parameters experimentally accessible. The values of the wave functions of the solitary waves at infinity in (3) are given by $\psi_{2\infty}^2 = (1 - \alpha - \Lambda^2)/(1 - \alpha^2)$ and $\psi_{1\infty}^2 = 1 - \alpha\psi_{2\infty}^2$. In the long-wave limit ($k \rightarrow 0$), (4) gives two acoustic branches $\omega_{\pm} \approx c_{\pm} k$ with the corresponding sound velocities $c_{\pm}^2 = \frac{1}{4}(\psi_{1\infty}^2 + \psi_{2\infty}^2 \pm \sqrt{(\psi_{1\infty}^2 - \psi_{2\infty}^2)^2 + 4\alpha^2 \psi_{1\infty}^2 \psi_{2\infty}^2})$. The solitary waves I seek below are all subsonic, i.e., $U < c_-$. This gives a restriction on the asymmetry parameter Λ^2 : c_- is real only if $\Lambda^2 < 1 - \alpha$.

Each solitary wave complex that belongs to a family of the solitary wave solutions for a chosen set of (α, Λ^2) will be characterized by its velocity U , vortex radii b_i , momenta $\mathbf{p}_i = (0, 0, p_i)$, and energy \mathcal{E} . The momentum (or impulse) of the i th component is $\mathbf{p}_i = \frac{1}{2i} \int [(\psi_i^* - \psi_{i\infty}) \nabla \psi_i - (\psi_i - \psi_{i\infty}) \nabla \psi_i^*] dV$. The reasons for replacing a more customary defined momentum $\hat{\mathbf{p}}_i = \frac{1}{2i} \int \psi_i^* \nabla \psi_i - \psi_i \nabla \psi_i^* dV$ with the convergent integrals \mathbf{p}_i were spelled out in [6] for a one-component GP equation. Also, similar to [6], we form the energy \mathcal{E} by subtracting the energy of an undisturbed system of the same mass for which $\psi_i = \text{const}$ everywhere, from the energy of the system with a solitary wave, so that the energy of the system becomes

$$\begin{aligned} \mathcal{E} &= \frac{1}{2} \sum_{i=1}^2 \int \left\{ |\nabla \psi_i|^2 + \frac{1}{2} (\psi_{i\infty}^2 - |\psi_i|^2)^2 \right\} dV \\ &+ \frac{\alpha}{2} \int \prod_{i=1}^2 (\psi_{i\infty}^2 - |\psi_i|^2) dV. \end{aligned} \quad (5)$$

By performing the variation $\psi_i \rightarrow \psi_i + \delta\psi_i$ in the integrals for \mathcal{E} and p_i , discarding surface integrals that vanish provided $\delta\psi_i \rightarrow 0$ for $|\mathbf{x}| \rightarrow \infty$ and making use of (3), we obtain $\delta\mathcal{E} = U\delta(p_1 + p_2)$, or $U = \partial\mathcal{E}/\partial(p_1 + p_2)$, where the derivative is taken along the solitary wave sequence. The same expression is obeyed by the sequences of clas-

TABLE I. The velocity U , energy \mathcal{E} , momenta p_i , and radii, b_i , of the solitary wave solutions of (3) with $\alpha = 0.05$ and $\Lambda^2 = 0.1$. The sequence terminates at $U = c_- \approx 0.646$.

U	\mathcal{E}	p_1	p_2	b_1	b_2	complex
0.55	118	92.3	80.8	1.83	1.50	VR-VR
0.58	107	81.0	72.6	1.47	0.57	VR-VR
0.60	101	74.9	69.6	1.12	...	VR-RP
0.63	102	66.2	79.0	RP-RP

sical vortex rings in an incompressible fluid and by the solitary waves of [6]. By applying some algebraic manipulations that involve some integration by parts, the following integral properties were established:

$$\mathcal{E} = \int \left| \frac{\partial \psi_1}{\partial z} \right|^2 + \left| \frac{\partial \psi_2}{\partial z} \right|^2 dV, \quad (6)$$

$$\mathcal{E} = \int \sum_{i=1}^2 f_i(\psi_1, \psi_2) [2\psi_{i\infty}^2 - \psi_{i\infty}(\psi_i + \psi_i^*)] dV \quad (7)$$

$$2U \sum_{i=1}^2 p_i = \int \sum_{i=1}^2 f_i(\psi_1, \psi_2) \times [3\psi_{i\infty}^2 - \psi_{i\infty}(\psi_i + \psi_i^*) - |\psi_i|^2] dV \quad (8)$$

where $f_1(\psi_1, \psi_2) = (1 - |\psi_1|^2 - \alpha|\psi_2|^2)/2$ and $f_2(\psi_1, \psi_2) = (1 - \alpha|\psi_1|^2 - |\psi_2|^2 - \Lambda^2)/2$. These were used as checks on numerical accuracy of the solutions I obtain next.

The axisymmetric solitary waves are found by rewriting (3) in cylindrical coordinates (s, θ, z) for the deviations from the solutions at infinity $\Psi_i = \psi_i - \psi_{i\infty}$. Stretched variables $z' = z$ and $s' = s\sqrt{1 - 2U^2}$ were introduced and the infinite domain was mapped onto the box $(0, \frac{\pi}{2}) \times (-\frac{\pi}{2}, \frac{\pi}{2})$ using the transformation $\hat{z} = \tan^{-1}(Dz')$ and $\hat{s} = \tan^{-1}(Ds')$, where $D \sim 0.4-0.5$. Transformed Eqs. (3) were expressed in second-order finite difference form using 100^2 grid points, and the resulting nonlinear equations were solved by Newton-Raphson iteration procedure using banded matrix linear solver based on bi-conjugate gradient stabilized iterative method with preconditioning. As $\alpha \rightarrow 0$, two components become uncoupled, so the solitary wave sequence for each component is following the dispersion curve of the one-component GP equation (1) with vortex rings (VRs) becoming rarefaction pulses (RPs) as U increases, with energy and momentum being appropriately scaled by the densities at infinity. For $\alpha \neq 0$, different components become RP at different critical values of U , so a variety of complexes becomes possible. Table I gives an example of various transitions from one complex to another in the system with $\alpha = 0.05$ and $\Lambda^2 = 0.1$. Notice that the radii of the vortex rings in VR-VR complexes differ with $b_2 \rightarrow b_1$ as $U \rightarrow 0$. Also notice, that there is a cusp in the dispersion curve \mathcal{E} vs $p_1 + p_2$, since the solitary wave complex moving with $U = 0.63$ belongs to the upper branch.

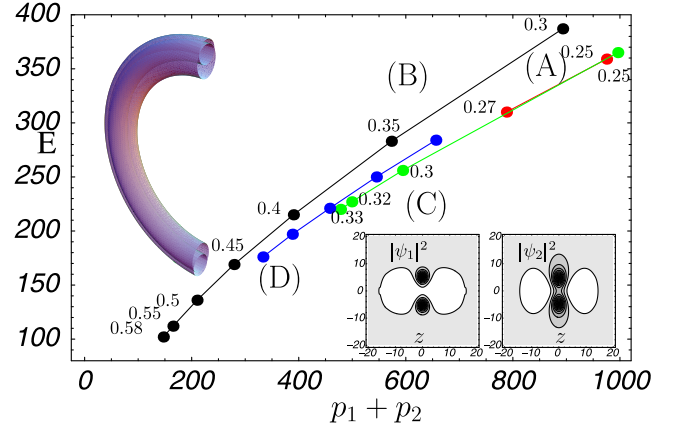


FIG. 1 (color online). The dispersion curves of four families of the axisymmetric solitary wave solutions of (3) (A) (red line) $\alpha = 0.7$ and $\Lambda^2 = 0.1$ ($c_- = 0.2738$); (B) (black line) $\alpha = 0.1$ and $\Lambda^2 = 0.1$ ($c_- = 0.6169$); (C) (green line) $\alpha = 0.5$ and $\Lambda^2 = 0.25$ ($c_- = 0.3317$); (D) (blue line) $\alpha = 0.5$ and $\Lambda^2 = 0.1$ ($c_- = 0.3905$). The numbers next to the dots give the velocity of the corresponding solitary wave. For (D) (blue line) these are 0.3, 0.32, 0.34, 0.36, 0.38. All these solutions are VR-VR complexes except for $U = 0.58$ on (B) branch which is VR-RP. The top inset shows the density isosurface at $|\psi_1|^2 = \frac{1}{10}\psi_{1\infty}^2$ and $|\psi_2|^2 = \frac{1}{10}\psi_{2\infty}^2$ for a half of the VR-VR complex for $\alpha = 0.5$, $\Lambda^2 = 0.25$ that is moving with $U = 0.3$. The radii are $b_1 = 5.194$ and $b_2 = 4.796$. The density contour plots of this solution are shown in the bottom inset.

As the interaction strength α increases for fixed Λ^2 and U , the radii in VR-VR complexes do not change much, although energy and momentum decrease significantly. We can compare two such solutions for $\Lambda^2 = 0.1$ and $U = 0.3$: the VR-VR complex for $\alpha = 0.1$ has $\mathcal{E} = 387$, $p_1 = 484$, $p_2 = 410$, $b_1 = 5.197$, and $b_2 = 5.096$, whereas for $\alpha = 0.5$ these values are $\mathcal{E} = 284$, $p_1 = 385$, $p_2 = 271$, $b_1 = 5.196$, and $b_2 = 5.093$. On the other hand, if α and U are kept constant and the asymmetry parameter Λ^2 increases, the radius of the vortex ring in the second component decreases (if $\Lambda^2 = 0.5$, $\alpha = 0.1$, $U = 0.3$, then

TABLE II. The intercomponent interaction strength α , energy \mathcal{E} , momenta p_i , and radii b_i , of the solitary wave solutions of (3) with $U = 0.3$ and $\Lambda^2 = 0.1$. The sequence terminates ($c_- = U$) at $\alpha \approx 0.65$.

α	\mathcal{E}	p_1	p_2	b_1	b_2	complex
0.2	178	414	1.52	4.977	...	VR-SW
0.4	142	330	7.76	4.673	...	VR-SW
0.6	119	268	35.1	4.122	...	VR-SW
α	\mathcal{E}	p_1	p_2	b_1	b_2	complex
0.2	140	1.12	330	...	4.787	SW-VR
0.4	96.7	4.89	237	...	4.354	SW-VR
0.6	63.0	17.5	174	...	2.986	SW-VR

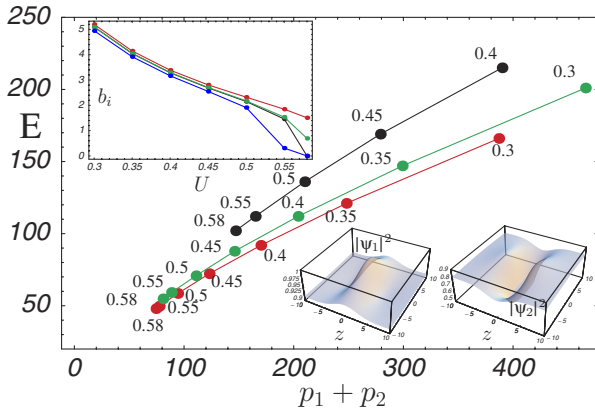


FIG. 2 (color online). The dispersion curves of three families of the axisymmetric solitary wave solutions of (3) with $\alpha = 0.1$ and $\Lambda^2 = 0.1$. The numbers next to the dots give the velocity of the solitary wave solution. The top (black) branch corresponds to VR-VR (VR-RP for $U = 0.58$) complexes. The middle (green) branch shows p vs \mathcal{E} for VR-SW complexes and the bottom (red) branch is the dispersion curve of SW-VR (SW-RP for $U = 0.58$) complexes. The radii of the vortex ring solutions are shown on the upper inset as a function of U : the two top (red and green) lines give b_1 and b_2 correspondingly for VR-VR complexes. The two bottom (black and blue) lines represent b_1 in VR-SW complex and b_2 in SW-VR complex, respectively. The bottom inset shows 3D plots of $|\psi_i(s, z)|^2$ of the SW-RP complex moving with the velocity $U = 0.58$.

$\mathcal{E} = 284$, $p_1 = 503$, $p_2 = 160$, $b_1 = 5.182$, and $b_2 = 4.363$). Figure 1 shows the dispersion curves of families of the axisymmetric solitary wave complexes for a variety of (α, Λ^2) .

In addition to the VR-VR, VR-RP, and RP-RP complexes that I have just described, two other families of the solitary waves came as a surprise. In contrast with the VR-VR, VR-RP, and RP-RP complexes, in which the solitary wave in each component possesses a large momentum, the total momentum of the system in the new families almost entirely belongs to one component with the disturbance of the other component moving almost entirely through the coupling with the mobile component. I will call this disturbance a “slaved wave” (SW). This gives rise to two other complexes such as VR-SW and RP-SW. Notice that the role of the components can be reversed giving SW-VR and SW-RP complexes as well. To indicate how the characteristics of these complexes change with increasing intercomponent interaction strength α , the parameters of these solutions are given in Table II for $U = 0.3$ and $\Lambda^2 = 0.1$. Figure 2 shows the dispersion curves of all three families of the axisymmetric solitary wave solutions for $\alpha = 0.1$ and $\Lambda^2 = 0.1$.

Finally, when the solitary waves are found, there is a need to elucidate the following topics. (i) *Stability*.—The Derrick-type argument used in [6] can be applied together with the integral identities (5)–(8), to suggest the stability of solitary waves as long as $\partial U / \partial (p_1 + p_2) < 0$ along the family. This condition is satisfied for all solitary waves discussed here except for the last entry of Table I. (ii) *Solitary waves in 2D*.—Similarly to 3D complexes, solitary waves in 2D consist of the combinations of a pair of two vortices with opposite circulation (VP), 2D rarefaction pulse, or a slaved wave, giving rise to VP(RP)-VP(RP) and SW-VP(RP) complexes. (iii) *Formation*.—The mechanisms of solitary wave nucleation in two-component condensates are similar to those in one-component condensates [11]. In particular, the moving objects (ions, laser beams, etc.) shed these complexes during a transonic transition. I will elaborate on these issues in detail elsewhere.

The support from NSF grant no. DMS-0104288 is acknowledged.

-
- [1] G. Volovik, *The Universe in a Helium Droplet* (Clarendon Press, Oxford, 2003).
 - [2] G. Modugno *et al.*, *Science* **294**, 1320 (2001).
 - [3] C. J. Myatt, E. A. Burt, R. W. Ghrist, E. A. Cornell, and C. E. Wieman, *Phys. Rev. Lett.* **78**, 586 (1997).
 - [4] B. D. Esry and C. H. Greene, *Phys. Rev. A* **57**, 1265 (1998); Th. Busch *et al.*, *Phys. Rev. A* **56**, 2978 (1997); B. D. Esry *et al.*, *Phys. Rev. Lett.* **78**, 3594 (1997); T. L. Ho, *Phys. Rev. Lett.* **81**, 742 (1998).
 - [5] V. L. Ginzburg and L. P. Pitaevskii, *Sov. Phys. JETP* **7**, 858 (1958); E. P. Gross, *Nuovo Cimento* **20**, 454 (1961); L. P. Pitaevskii, *Sov. Phys. JETP* **13**, 451 (1961).
 - [6] C. A. Jones and P. H. Roberts, *J. Phys. A* **15**, 2599 (1982); C. A. Jones, S. J. Putterman, and P. H. Roberts, *J. Phys. A* **19**, 2991 (1986).
 - [7] P. Öhberg and L. Santos, *Phys. Rev. Lett.* **86**, 2918 (2001); Th. Busch and J. R. Anglin, *Phys. Rev. Lett.* **87**, 010401 (2001); P. G. Kevrekidis *et al.*, *Eur. Phys. J. D* **28**, 181 (2004).
 - [8] S. Coen and M. Haelterman, *Phys. Rev. Lett.* **87**, 140401 (2001).
 - [9] J. Ruostekoski and J. R. Anglin, *Phys. Rev. Lett.* **86**, 3934 (2001); C. M. Savage and J. Ruostekoski, *Phys. Rev. Lett.* **91**, 010403 (2003); R. A. Battye, N. R. Cooper and P. M. Sutcliffe, *Phys. Rev. Lett.* **88**, 080401 (2002).
 - [10] K. Kasamatsu, M. Tsubota, and M. Ueda, *Phys. Rev. Lett.* **91**, 150406 (2003); K. Kasamatsu, M. Tsubota, and M. Ueda, *Phys. Rev. Lett.* **93**, 250406 (2004).
 - [11] N. G. Berloff, *Phys. Rev. A* **69**, 053601 (2004); N. G. Berloff, *J. Phys. A* **37**, 1617 (2004).